



Characterization of deep impurities in semiconductors by terahertz tunneling ionization

S.D. Ganichev^{a,b,*}, E. Ziemann^a, I.N. Yassievich^b, V.I. Perel^b, W. Prettl^a

^a*Institut für Exp. und Angew. Physik, Universität Regensburg, 93040 Regensburg, Germany*

^b*A. F. Ioffe Physicotechnical Institute of the RAS, 194021 St. Petersburg, Russia*

Abstract

Tunneling ionization in high-frequency fields as well as in static fields is suggested as a method for the characterization of deep impurities in semiconductors. It is shown that an analysis of the field and temperature dependences of the ionization probability allows to obtain defect parameters like the charge of the impurity, tunneling times, the Huang–Rhys parameter, the difference between optical and thermal binding energy and the basic structure of the defect adiabatic potentials. Compared to static fields, high-frequency electric fields in the terahertz-range offer various advantages, as they can be applied contactlessly and homogeneously even to bulk samples using the intense radiation of a high-power pulsed far-infrared laser. © 2001 Elsevier Science Ltd. All rights reserved.

Keywords: Deep impurities; Terahertz radiation; Tunneling

1. Introduction

Investigation of the effect of an electric field on thermal ionization and trapping of carriers has been widely used to probe deep impurities in semiconductors. The standard method for the characterization of deep centers is DLTS [1] which is applied in various modifications. Here we will show that the investigation of phonon-assisted tunneling in strong static or alternating electric fields, in particular of terahertz frequencies, can be used to obtain the parameters of multiphonon transitions determining the nonradiative recombination rate.

2. Tunneling ionization in alternating electric fields

The application of strong electric fields to semiconductors with deep centers leads to the stimulation of

ionization/capture processes due to the Poole–Frenkel effect, phonon-assisted tunneling and direct tunneling. The Poole–Frenkel effect occurs for charged impurities only and can be observed for relatively small electric field, whereas all types of impurities can be ionized by tunneling. The phonon-assisted tunneling in static electric fields was first studied numerically in [2]. In semiclassical approximation the ionization probability $e(E)$ of deep neutral centers due to phonon-assisted tunneling in an alternating electric field $\vec{E}(t) = E \cos(\omega t)$ is given by [3]

$$e(E) = e(0) \exp\left[\frac{E^2}{(E_c^*)^2}\right] \quad \text{with} \quad (E_c^*)^2 = \frac{3m^* \hbar}{e^2(\tau_2^*)^3}, \quad (1)$$

where m^* is the effective mass of the carrier and τ_2^* is an effective time:

$$(\tau_2^*)^3 = \frac{3}{4\omega^3} (\sinh(2\omega\tau_2) - 2\omega\tau_2). \quad (2)$$

The tunneling time τ_2 is given by

$$\tau_2 = \frac{\hbar}{2k_B T} \pm \tau_1, \quad \tau_1 = \frac{1}{2\omega_{\text{vib}}} \left| \ln \frac{\varepsilon_T}{\varepsilon_{\text{opt}} - \varepsilon_T} \right|, \quad (3)$$

where T is the temperature, ω_{vib} is the impurity vibration frequency, ε_{opt} and ε_T are the optical and

*Correspondence address: Institut für Exp. und Angew. Physik, Universität Regensburg, 93040 Regensburg, Germany. Tel.: +49-941-943-2050; fax: +49-941-943-4223.

E-mail address: sergey.ganichev@physik.uni-regensburg.de (S.D. Ganichev).

thermal ionization energies, respectively. The plus and minus signs in Eq. (3) correspond to the adiabatic potential structures of substitutional impurities (top left in Fig. 2) and autolocalized impurities (bottom right in Fig. 2), respectively.

The electric field and temperature dependences of the ionization probability allow to deduce deep impurity parameters according to Eqs. (1)–(3). This may be done in the quasi-static limit $\omega\tau_2 \ll 1$ most conveniently. In this limit the effective time τ_2^* in Eq. (1) becomes equal to the defect tunneling time τ_2 yielding an ionization probability independent of ω . Thus, τ_2 may be determined directly from the slope of $\ln(e(E)/e(0))$ as a function of E^2 . Comparing τ_2 with the value of $\hbar/(2k_B T)$ allows to conclude on the basic structure of the defect adiabatic potentials and yields τ_1 according to Eq. (3). From values of the tunneling time τ_1 , Eq. (3) leads to the impurity vibration frequency ω_{vib} , if ε_{opt} and ε_T are known, or vice versa to the difference $\Delta\varepsilon = \varepsilon_{\text{opt}} - \varepsilon_T$, if ω_{vib} and ε_T are known.

3. Experimental

Terahertz electric fields have been applied to semiconductor samples by illumination with an optically

pumped powerful far-infrared molecular gas laser. Using NH_3 , CH_3F , and D_2O as laser media 40 ns pulses have been achieved at wavelengths of 76, 90, 148, 280, 385, and 496 μm with the intensity up to 5 MW/cm^2 [4]. The pump radiation source was a tunable TEA CO_2 -laser commercially available. Two basically different kinds of deep impurity centers in semiconductors have been studied: (i) substitutional impurities with weak electron–phonon coupling and (ii) autolocalized centers (DX-centers in A_3B_5 alloys) with strong electron–phonon coupling (see Table 1, for more details see [5]). Samples were cooled to $T = 4.2\text{--}200 \text{ K}$ where practically all carriers are frozen out on the impurity. The normalized emission rate $e(E)/e(0)$ has been measured by photoconductivity using a standard electric circuit. The laser pulse duration was shorter than the carrier capture time. Thus, recombination during the excitation can be ignored and the ratio of the conductivity under illumination and in the dark, σ_i/σ_d , is proportional to $e(E)/e(0)$.

4. Experimental results and discussion

A photoconductive signal increasing nonlinearly with incident power has been observed for all samples in spite

Table 1
Parameters of samples investigated

	ε_T (meV)	ε_{opt} (meV)	$\Delta\varepsilon$ (meV)	τ_1 (s)	ω_{vib} (s^{-1})	S_{HR}
AlGaAs:Te	140	850	710	3.3×10^{-15}	2.5×10^{14}	4
AlGaSb:Te	120	860	740	2.9×10^{-14}	3.0×10^{13}	36
Ge: Au	150	160	10	4.5×10^{-14}	3.0×10^{13}	0.5
Ge: Hg	90	106	16	2.9×10^{-14}	2.7×10^{13}	0.8
Ge: Cu	40	—	—	4.1×10^{-14}	—	—

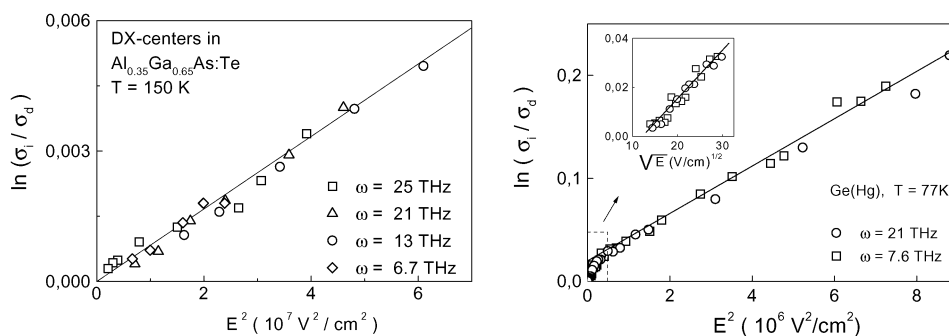


Fig. 1. Logarithm of the ionization probability, given by the ratio $\ln(\sigma_i/\sigma_d) = \ln(e(E)/e(0))$ plotted as a function of E^2 . Left plate: DX-centers in $\text{Al}_{0.35}\text{Ga}_{0.65}\text{As}:\text{Te}$ at $T = 150 \text{ K}$. Right plate: $\text{Ge}:\text{Hg}$ plotted at $T = 77 \text{ K}$. Inset: ionization probability as a function of the square root of the electric field.

of the fact that the photon energies were much smaller than the binding energy of the impurities. Fig. 1 (left plate) shows an example obtained for DX-centers in Te-doped AlGaAs at $T = 150$ K. The logarithm of σ_i/σ_d is plotted as a function of the square of the electric field strength of laser pulses. The probability of electron detachment from the deep center is independent on the radiation frequency and increases exponentially with the E^2 . DX-centers in AlGaAs have been chosen to demonstrate the proposed method because this material shows phonon-assisted tunneling beginning with zero electric field up to rather high electric field strengths. The slope of $\ln(\sigma_i/\sigma_d)$ as a function of E^2 gives the characteristic field E_c^* and the effective time τ_2^* can be calculated using Eq. (1). As the ionization probability is independent on the field frequency, $\tau_2^* = \tau_2$ at all frequencies used here. Fig. 1 (right plate) shows the ionization probability of singly charged substitutional impurities (Ge:Hg) as a function of E^2 at $T = 77$ K in a lin–log plot. Here, the straight line in the $\ln(e(E)/e(0))$ vs. E^2 diagram is shifted along the ordinate to higher values. This increase of the phonon-assisted tunneling probability for charged impurities is caused by the lowering of the Coulomb potential barrier height [4]. At lower fields strength the Poole–Frenkel effect dominates carrier emission and the ionization probability exponentially grows with \sqrt{E} (see inset in Fig. 1, left plate) [6]. Thus, to determine the charge state of an impurity, two criteria can be used: (i) observation of the Poole–Frenkel effect at low fields and (ii) the shift of the straight line in the $\ln(e(E)/e(0))$ vs. E^2 diagram at higher electric fields where phonon-assisted tunneling causes ionization. For the second criterion it is essential to normalize the dependence $e(E)$ by the emission probability at zero electric field, $e(0)$.

Analogous results have been obtained from several donor- and acceptor-doped semiconductors. Fig. 2 presents the temperature dependence of the tunneling time τ_2 obtained for various samples in the quasi-static regime ($\omega\tau_2 < 1$) of phonon-assisted tunneling. For the purpose of comparison, $\hbar/(2k_B T)$ is also plotted in Fig. 2. As can be seen, τ_2 is larger than $\hbar/(2k_B T)$ for substitutional impurities and smaller than $\hbar/(2k_B T)$ for the DX-centers. Thus, the tunneling time compared to $\hbar/(2k_B T)$ reflects the basic structure of the potential barriers which is systematically distinct for both potential configurations discussed here and shown in the insets in Fig. 2. From τ_2 and the temperature T , the value of τ_1 can be obtained using Eq. (3). The results are given in Table 1. After Eq. (3), τ_1 links the impurity thermal and optical binding energies with the local vibration frequency. As for DX-centers the values of ε_T and ε_{opt} are known from literature, determination of τ_1 allows to derive the local vibration frequency. For Ge:Hg ω_{vib} is known [7] as well as ε_T . With these data and the knowledge of τ_1 , the difference between the

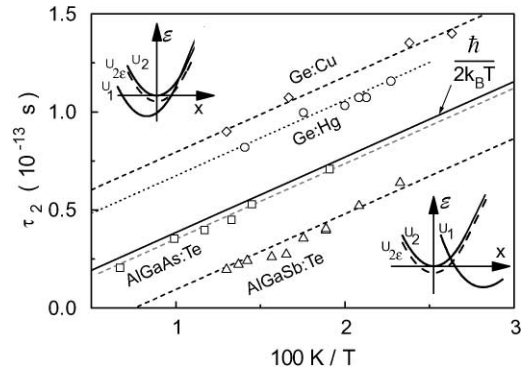


Fig. 2. Tunneling times τ_2 as a function of $1/T$. The full line shows $\hbar/2k_B T$, the broken lines are plotted according to Eq. (3). The values for τ_1 are given in Table 1. Insets: Adiabatic potentials for substitutional impurities (top left) and auto-localized impurities (bottom right).

optical and the thermal binding energies $\Delta\varepsilon = \varepsilon_{opt} - \varepsilon_T$ can be determined. Finally, we note that these data can also be represented by the frequently used Huang–Rhys parameter $S_{HR} = \Delta\varepsilon/\hbar\omega_{vib}$ and the electron–phonon interaction parameter $\beta = \Delta\varepsilon/\varepsilon_T$.

At high electric fields phonon-assisted tunneling proceeds into direct tunneling and a weaker growth of ionization probability is observed compared to the field dependence of phonon-assisted tunneling extrapolated to higher fields [4]. The transition field strength E_{trans} [4] strongly depends on $\Delta\varepsilon = \varepsilon_{opt} - \varepsilon_T$ and ω_{vib} and allows to determine these parameters. With decreasing temperature E_{trans} shifts to lower field strengths. Therefore, e.g. at 4.2 K, the field strength where phonon-assisted tunneling occurs may be so small that the exponential E^2 -dependence of the ionization probability gets very hard to be detected. The direct tunneling sets a lower limit of the temperature and an upper limit of the electric field strength for the proposed method of deep impurity analysis.

Finally, we would like to emphasize that the analysis presented here is only valid in the quasi-static limit, i.e. for frequencies less than τ_2^{-1} . At $\omega\tau_2 > 1$, a strong frequency dependence of the ionization probability has been observed (Eq. (1)) [3].

5. Conclusion

Terahertz ionization of deep impurities in semiconductors has been proposed as a method for the characterization of deep impurities. All measurements carried out with terahertz radiation but in the quasi-static regime may as well be performed using

static electric fields like in DLTS. The proposed method of impurity ionization by short far-infrared laser pulses permits contactless application of very strong electric fields to samples. The high sensitivity of the photoconductive response offers a possibility of measurements over a broad field range, from tens of kV/cm to very low field strengths.

Acknowledgements

Financial support by the DFG, the RFFI and NATO Linkage Grant is gratefully acknowledged.

References

- [1] Lang DV. *J Appl Phys* 1974;45:3014.
- [2] Makram-Ebeid S, Lannoo M. *Phys Rev B* 1982;25:6406.
- [3] Ganichev SD, Ziemann E, Gleim Th, Prettl W, Yassievich IN, Perel VI, Wilke I, Haller EE. *Phys Rev Lett* 1998;80:2409.
- [4] Ganichev SD, Prettl W, Yassievich IN. *Phys Solid State* 1997;39:1703.
- [5] Ziemann E, Ganichev SD, Yassievich IN, Prettl W. *J Appl Phys* 2000;87:3843.
- [6] Ganichev SD, Ziemann E, Prettl W, Yassievich IN, Istratov AA, Weber ER. *Phys Rev B* 2000;61:10361.
- [7] Pakhomov AA, Polupanov AF, Galiev VI, Imamov EZ. *Sov Phys Solid State* 1991;33:416.